

# In Silico Analysis of Fluoroquinolone Derivatives as Inhibitors of Bacterial DNA Gyrase <sup>†</sup>

Evelin Jadán <sup>1,\*</sup>, Juan Diego Guarimata <sup>2</sup> and Javier Santamaría-Aguirre <sup>3,\*</sup><sup>1</sup> Facultad de Ciencias Químicas (FCQ), Universidad Central del Ecuador (UCE), Quito 170521, Ecuador<sup>2</sup> CEQUINOR (UNLP-CONICET, CCT La Plata, Associated with CIC PBA), Departamento de Química, Facultad de Ciencias Exactas, Universidad Nacional de la Plata, La Plata B1900, Argentina; juanguarimata@quimica.unlp.edu.ar<sup>3</sup> Facultad de Ciencias Químicas (FCQ), Universidad Central del Ecuador (UCE), Grupo de Investigación en Biodiversidad, Zoonosis y Salud Pública (GIBCIZ), Quito 170521, Ecuador

\* Correspondence: enjadan@uce.edu.ec (E.J.); jrsantamaria@uce.edu.ec (J.S.-A.)

<sup>†</sup> Presented at the 29th International Electronic Conference on Synthetic Organic Chemistry (ECSOC-29); Available online: <https://sciforum.net/event/ecsoc-29>.

## Abstract

Antimicrobial resistance represents a growing threat to global public health [1]. The indiscriminate use of antibiotics has accelerated the emergence of resistant strains, reducing the therapeutic effectiveness of currently available drugs, fluoroquinolones being no exception [2,3]. In this context, the design of new antimicrobials remains a significant challenge. This study evaluated, using in silico tools, the binding affinity of eight novel fluoroquinolone derivatives against the DNA gyrase of six bacterial species, using moxifloxacin as the reference compound. Target protein sequences were retrieved from the Protein Data Bank and GenBank and subsequently modeled using SwissModel, I-TASSER, and Phyre2. The generated structures were assessed with MolProbity, and those with the best scores were selected for molecular docking. Proteins were prepared using Chimera 1.18 and AutoDockTools 1.5.7. The active site was identified with Discovery Studio 2024. Ligands were built in ZINC, prepared using Open Babel v3.1.1.60, and docked with AutoDock Vina v1.2.3.57. Docking validation was performed with DockRMSD. Considering these results, four new molecules (A1, B1, C1, and D2) were designed to improve their pharmacokinetic properties by modifying the TPSA value of the original structures. However, the new docking assays revealed that these optimized compounds did not exhibit a significant increase in affinity toward the target enzyme. The findings suggest that compound C retains a favorable profile as a potential antimicrobial agent against resistant strains.

**Keywords:** antimicrobial resistance; fluoroquinolone derivatives; molecular docking; DNA gyrase

Academic Editor(s): Name

Published: date

**Citation:** Jadán, E.; Guarimata, J.D.; Santamaría-Aguirre, J. In Silico Analysis of Fluoroquinolone Derivatives as Inhibitors of Bacterial DNA Gyrase. *Chem. Proc.* **2025**, volume number, x. <https://doi.org/10.3390/xxxxx>

**Copyright:** © 2025 by the authors. Submitted for possible open access publication under the terms and conditions of the Creative Commons Attribution (CC BY) license (<https://creativecommons.org/licenses/by/4.0/>).

## 1. Introduction

Antimicrobial resistance (AMR) has emerged as a significant global health threat, compromising the effectiveness of antibiotics and restricting therapeutic options. The widespread use of antimicrobial agents over the last century has accelerated the emergence of resistance mechanisms, posing a serious challenge to public health [1–3]. Current treatments are becoming increasingly ineffective against multidrug-resistant (MDR)

bacteria, while the demand for new antibiotics continues to grow [1]. Among the most concerning pathogens are the so-called ESKAPE organisms—*Enterococcus faecium*, *Staphylococcus aureus*, *Klebsiella pneumoniae*, *Acinetobacter baumannii*, *Pseudomonas aeruginosa*, and *Enterobacter* spp.—which represent the leading cause of hospital-acquired infections worldwide and are associated with high rates of morbidity and mortality [1,2].

Fluoroquinolones are broad-spectrum antimicrobials widely used in clinical practice. Their primary mode of action is the inhibition of bacterial DNA synthesis [4]. The cellular targets of these agents are two essential bacterial enzymes, DNA gyrase (topoisomerase II) and topoisomerase IV, which play crucial roles in DNA replication and transcription [2,4–6]. Resistance to fluoroquinolones has emerged through various mechanisms, including target-site mutations that reduce drug binding, increased expression of efflux pumps, and the acquisition of resistance-conferring genes [2,4]. Mutations in DNA gyrase and topoisomerase IV typically cluster within a conserved domain of the GyrA and ParC subunits, known as the quinolone resistance-determining region (QRDR). In *Escherichia coli*, this region spans amino acids 67–106 in GyrA and 63–102 in ParC, and mutations within this domain markedly decrease drug affinity for the DNA–enzyme complex [4,7].

Despite the clinical success of fluoroquinolones, the quinolone scaffold remains an attractive framework for further chemical optimization. Structural modifications hold potential for improving pharmacokinetic and pharmacodynamic properties, thereby broadening their therapeutic utility [2]. In this context, molecular docking has emerged as a powerful in silico tool to explore drug–target interactions. This approach enables the prediction of binding affinities and modes of interaction between small molecules and protein targets, providing valuable insights into the biochemical processes underlying drug action [8].

The present study aimed to evaluate, through computational approaches, the binding affinity of newly designed fluoroquinolone derivatives against DNA gyrase from *E. coli*, *K. pneumoniae*, *Salmonella infantis*, *S. enteritidis*, *S. aureus*, and *Mycobacterium tuberculosis*.

## 2. Materials and Methods

### 2.1. Protein Retrieval and Modeling

The crystal structures of gyrases from *E. coli* in complex with the co-crystallized ligand MFX (Moxifloxacin) (PDB ID: 9GGQ), *S. aureus* (PDB ID: 5NPP), and *M. tuberculosis* (PDB ID: 5BS8) were retrieved in PDB format from the Protein Data Bank (PDB) (<http://www.rcsb.org>) [9]. For *K. pneumoniae* (A0A485SP94), *S. infantis* (A0A5U9GQ37), and *S. enteritidis* (ANF19453) structural models were generated from protein sequences obtained from UniProt (<https://www.uniprot.org/>) and Gen Bank (<https://www.ncbi.nlm.nih.gov/genbank/>) [10,11]. Homology modeling was performed using four servers: I-TASSER (<https://zhanggroup.org/I-TASSER/>) [12], Swiss-Model (<https://swissmodel.expasy.org/>) [13], and Phyre2 (<http://www.sbg.bio.ic.ac.uk/~phyre2/html/page.cgi?id=index>) [14]. The resulting models were evaluated using MolProbity (<http://molprobity.biochem.duke.edu/>) [15], and the best-scoring structures were selected for further analyses.

### 2.2. Protein Preparation

For modeled proteins, DNA chains and Mg<sup>2+</sup> ions were incorporated using Discovery Studio Visualizer 2024, extrapolating their position from the crystallized *E. coli* structure with Chimera v1.18. The processed structures were saved in PDB format. For crystallographic proteins, water molecules and non-essential ions were removed using Chimera v1.18. Input files for docking simulations were prepared with AutoDock Tools v1.5.7,

where polar hydrogens and Kollman charges were added, AD4 atom type were assigned, and the final files were saved in PDBQT format.

### 2.3. Ligand Preparation

Ligand SMILES codes were obtained from the ZINC database (<https://zinc.docking.org/>) [16]. The ligands were converted into 3D structures, protonated at pH 7.4, and energy-minimized using the UFF force field with Open Babel v3.1.1. The prepared ligands were exported in PDBQT format for docking analysis.

### 2.4. Docking and Validation

Docking simulations were performed with AutoDock Vina v1.2.3.57. The docking grid box was centered on the active site (coordinates:  $x = 207.75$ ,  $y = 220.194$ ,  $z = 225.083$ ) with dimensions of  $14 \times 24 \times 18 \text{ \AA}$ , covering the QRDR domain for *E. coli*. Ten conformations were generated for each ligand. Moxifloxacin was used as a reference compound, and docking validation was carried out through RMSD calculation using the DockRMSD server (<https://zhanggroup.org/DockRMSD/>) [17].

## 3. Results and Discussion

The docking protocol was validated by calculating the RMSD between the docked pose for moxifloxacin and its co-crystal structure with *E. coli*, yielding a value of 0.973, which falls within the accepted range for computational studies [18,19] and confirms the reliability of the methodology. The binding affinity of four in silico-designed fluoroquinolone derivatives (A-D) was evaluated against DNA gyrase from *E. coli*, *K. pneumoniae*, *S. infantis*, *S. enteritidis*, *S. aureus*, and *M. tuberculosis* (Figure 1). For each ligand, 10 conformations were generated, and the top-ranked pose was selected for analysis.

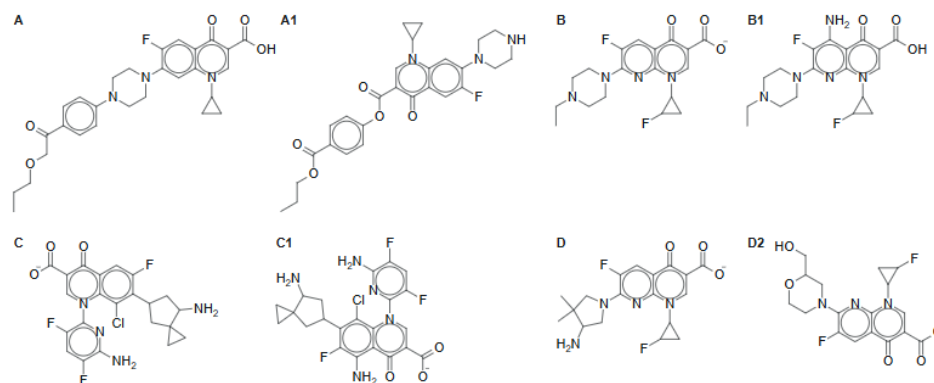


**Figure 1.** Molecular structures of the selected ligands.

The binding energies found ranged from  $-7.46$  to  $-17.88$  kcal/mol (Table 1), consistent with stable ligand–enzyme interactions. Compound **A** exhibited lower binding affinities than the control in most species, except for *S. aureus*, where it displayed stronger affinity ( $-11.30$  kcal/mol). Compound **B** showed a similar trend, with generally weaker affinities than the control, although its interaction with *K. pneumoniae* was comparable. In contrast, Compound **C** emerged as the most promising candidate, showing the strongest affinities across all bacterial species, surpassing the control in most cases, except for *M. tuberculosis*, where the binding affinity was similar ( $-17.52$  kcal/mol vs.  $-17.88$  kcal/mol). Compound **D** demonstrated lower affinities overall, but exceeded the control in *S. aureus* ( $-11.03$  kcal/mol) and showed comparable interaction with *K. pneumoniae*.

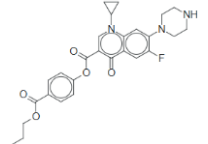
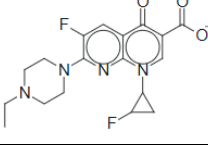
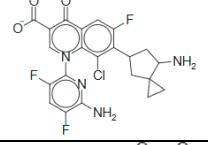
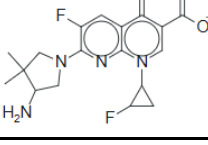
**Table 1.** Molecular docking results showing binding affinities (kcal/mol) of four in silico–designed fluoroquinolone derivatives (A–D) compared with moxifloxacin, against DNA gyrase.

|                       | <i>E. coli</i> | <i>S. enteritidis</i> | <i>S. infantis</i> | <i>K. pneumoniae</i> | <i>S. aureus</i> | <i>M. tuberculosis</i> |
|-----------------------|----------------|-----------------------|--------------------|----------------------|------------------|------------------------|
| <b>Moxifloxacin *</b> | −10.12         | −8.31                 | −8.39              | −8.29                | −9.27            | −17.88                 |
| <b>A</b>              | −9.63          | −7.53                 | −7.56              | −7.46                | −11.30           | −14.26                 |
| <b>B</b>              | −9.61          | −8.19                 | −8.17              | −8.62                | −8.69            | −17.14                 |
| <b>C</b>              | −12.14         | −9.19                 | −9.12              | −9.11                | −12.23           | −17.52                 |
| <b>D</b>              | −10.02         | −8.64                 | −8.24              | −8.63                | −11.03           | −17.85                 |

\*: control.

Analysis of binding interactions (Table 2) revealed the recurrent participation of residues located within the quinolone resistance-determining region (QRDR), particularly SER83 (Figure 2). Quinolone resistance has most commonly been associated with mutations in the amino-terminal domains of GyrA (residues 67 to 106 in *E. coli* numbering), with SER83 and ASP87 being the most frequent substitutions [4,20,21]. Additional stabilizing interactions were also observed, involving residues such as ARG121, GLY81, PTR129, and ARG128, depending on the bacterial species. These findings are consistent with previous reports describing mutations in GyrA and ParC as key contributors to reduced fluoroquinolone affinity [4,5,7]. Specifically, mutations at SER83 strongly affect fluoroquinolone binding to GyrA, whereas mutations at Arg121 do not exert the same impact [22]. Notably, Compound C established stronger and more diverse interactions with essential residues across all enzymes, correlating with its superior binding energies and suggesting enhanced robustness against resistance-associated mutations.

**Table 2.** Key amino acid residues involved in the interactions between fluoroquinolone derivatives (A–D) and DNA gyrase from the bacterial species analyzed, as predicted by molecular docking.

| Compound | Structure                                                                           | Key Residues      |                         |                         |                         |                  |                        |
|----------|-------------------------------------------------------------------------------------|-------------------|-------------------------|-------------------------|-------------------------|------------------|------------------------|
|          |                                                                                     | <i>E. coli</i>    | <i>S. enteritidis</i>   | <i>S. infantis</i>      | <i>K. pneumoniae</i>    | <i>S. aureus</i> | <i>M. tuberculosis</i> |
| <b>A</b> |  | GLY448<br>ARG121  | ASP82<br>SER83<br>ALA84 | ASP82<br>SER83          | ASP82<br>SER83          | ARG458<br>GLU435 | PTR129                 |
| <b>B</b> |  | LYS 447<br>ARG121 | ASP82<br>SER83<br>ALA84 | ASP82<br>SER83          | ASP82<br>SER83<br>ALA84 | ARG458           | ARG128                 |
| <b>C</b> |  | ASP426<br>ARG121  | GLY81                   | GLY81                   | GLY81                   | GLU435<br>ARG458 | ARG128<br>PTR129       |
| <b>D</b> |  | ASP426<br>ARG121  | GLY81                   | ASP82<br>SER83<br>ALA84 | ASP82<br>SER83<br>ALA84 | ARG458           | ARG128<br>PTR129       |

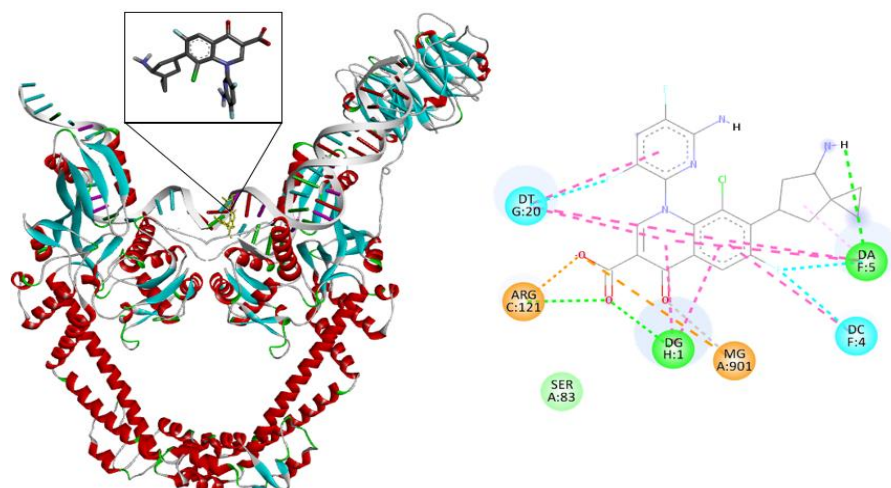


**Figure 2.** Interaction of GyrA of *E. coli* with the docked ligand C. Key interactions of C with protein residues include ARG121 and SER83. Figure generated using Discovery Studio Visualizer 2024.

These designed molecules were optimized to enhance their pharmacological profiles (Figure 1). In molecule A, the substituent at position C3 was removed to leave this site free and avoid interference with the FQ mechanism. In molecules B and C, one  $-NH_2$  group was introduced at position C5 to enhance pharmacokinetic properties and decrease the TPSA value—improving absorption in molecule B and preventing BBB penetration in molecule C. Finally, in molecule D, the substituent at position C7 was replaced with a 2-(hydroxymethyl)morpholin group.

Molecular docking analyses were conducted for the optimized molecules, and the corresponding binding affinities are summarized in Table 3. Overall, the affinity for the target pocket decreased across most bacterial species compared with previous results. This reduction was attributed to unfavorable ligand–enzyme interactions arising from the introduction of the amino group in molecules B and C. In molecule A, the substituent at position C7 also produced steric hindrance effects, generating unfavorable interactions due to its size. Nevertheless, a slight increase in binding affinity toward the GyrA subunit of *S. enteritidis* was observed for compounds A1 and B1, with B1 also exhibiting greater affinity for *S. aureus*. Conversely, compound D2 demonstrated a modest improvement in affinity for *S. infantis* relative to the original molecule D.

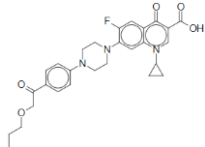
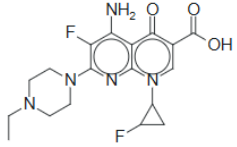
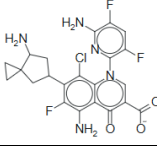
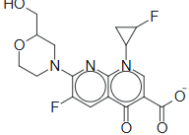
**Table 3.** Molecular docking scores (in kcal/mol) of optimized molecules against DNA gyrase.

|                       | <i>E. coli</i> | <i>S. enteritidis</i> | <i>S. infantis</i> | <i>K. pneumoniae</i> | <i>S. aureus</i> | <i>M. tuberculosis</i> |
|-----------------------|----------------|-----------------------|--------------------|----------------------|------------------|------------------------|
| <b>Moxifloxacin *</b> | −9.95          | −8.28                 | −8.31              | −8.28                | −9.37            | −17.72                 |
| <b>A1</b>             | −9.25          | −7.75                 | −7.35              | −7.47                | −6.02            | −11.14                 |
| <b>B1</b>             | −9.06          | −8.24                 | −7.79              | −7.92                | −9.46            | −15.16                 |
| <b>C1</b>             | −10.42         | −8.78                 | −8.77              | −8.76                | −11.11           | −16.54                 |
| <b>D2</b>             | −8.86          | −8.54                 | −8.35              | −7.93                | −9.37            | −15.69                 |

\*: control.

The interactions of the optimized molecules were generally consistent with those previously observed (Table 4). However, additional interactions were identified for compound A1, involving residues ALA119 and ALA118 in *E. coli*. In the case of *S. aureus*, an interaction with residue GLY459 was detected. All of these residues lie outside the QRDR region and are not associated with resistance arising from gyrase enzyme mutations.

**Table 4.** Key amino acid residues involved in the interactions between fluoroquinolone derivatives (A–D) and DNA gyrase from the bacterial species analyzed, as predicted by molecular docking.

| Compound  | Structure                                                                          | Key Residues   |                       |                    |                      |                  |                        |
|-----------|------------------------------------------------------------------------------------|----------------|-----------------------|--------------------|----------------------|------------------|------------------------|
|           |                                                                                    | <i>E. coli</i> | <i>S. enteritidis</i> | <i>S. infantis</i> | <i>K. pneumoniae</i> | <i>S. aureus</i> | <i>M. tuberculosis</i> |
| <b>A1</b> |   | ARG121         | ASP82                 | ASP82              | SER83                | GLY459           | PTR129                 |
|           |                                                                                    | ALA119         | SER83                 | SER83              | ALA84                | ARG458           | ALA125                 |
|           |                                                                                    | ALA118         | ALA84                 | ALA84              |                      | GLU435           |                        |
| <b>B1</b> |   | ARG121         | GLY81                 | GLY81              | GLY81                | GLY459           | ARG128                 |
|           |                                                                                    |                | SER83                 |                    |                      | ARG458           | PTR129                 |
|           |                                                                                    |                |                       |                    |                      | LEU457           |                        |
| <b>C1</b> |   | ARG121         | GLY81                 | GLY81              | GLY81                | ARG458           | ARG128                 |
|           |                                                                                    | SER83          | SER83                 | SER83              | SER83                | GLY436           | PTR129                 |
|           |                                                                                    |                |                       |                    |                      | GLU435           |                        |
| <b>D2</b> |  | ARG121         | ASP82                 | ASP82              | ASP82                |                  | ARG128                 |
|           |                                                                                    |                | SER83                 | SER83              | SER83                | ARG458           | PTR129                 |
|           |                                                                                    |                | ALA84                 | ALA84              | ALA84                |                  |                        |

The differences observed in the results underscore the structural diversity of each target enzyme and illustrate how this variability can be strategically exploited to combat antimicrobial resistance and enhance ligand affinity. These findings suggest that the structural modifications introduced in compound C not only decreased its binding affinity but also confer a distinct interaction profile across multiple bacterial species, an important attribute when targeting multidrug-resistant ESKAPE pathogens [23].

Collectively, these results establish compound C as a strong candidate for advanced preclinical evaluation, underscoring its selective antimicrobial potential and reduced likelihood of off-target effects on human topoisomerases. Nevertheless, the inherent limitations of docking studies should be acknowledged, as they do not account for protein conformational dynamics or the cellular environment. Future molecular dynamics simulations, complemented by in vitro and in vivo assays, will be essential to validate the therapeutic potential and safety of these derivatives [23–25].

**Author Contributions:** Conceptualization, J.S.-A.; methodology, E.J., and J.D.G.; software, E.J.; validation, E.J., J.D.G., J.S.-A.; formal analysis, E.J.; investigation, E.J.; data curation, E.J., writing—original draft preparation, E.J.; writing—review and editing, E.J., J.D.G., and J.S.-A.; visualization, E.J.; supervision, J.D.G. and J.S.-A.; All authors have read and agreed to the published version of the manuscript.

**Funding:** This research received no external funding.

**Institutional Review Board Statement:** Not applicable.

**Informed Consent Statement:** Not applicable.

**Data Availability Statement:** Not applicable.

**Acknowledgments:** Not applicable.

**Conflicts of Interest:** The authors declare no conflicts of interest.



## References

1. Kherroubi, L.; Bacon, J.; Rahman, K.M. Navigating fluoroquinolone resistance in Gram-negative bacteria: A comprehensive evaluation. *JAC-Antimicrob. Resist.* **2024**, *6*, dlae127. <https://doi.org/10.1093/jacamr/dlae127>.
2. Rodrigues, C.F.; Silva, F. The Rise, Fall, and Rethink of (Fluoro)quinolones: A Quick Rundown. *Pathogens* **2025**, *14*, 525. <https://doi.org/10.3390/pathogens14060525>.
3. Jakhar, R.; Khichi, A.; Kumar, D.; Dangi, M.; Chhillar, A.K. Discovery of novel inhibitors of bacterial DNA gyrase using a QSAR-Based approach. *ACS Omega* **2022**, *7*, 32665–32678. <https://doi.org/10.1021/acsomega.2c04310>.
4. Hooper, D.C.; Jacoby, G.A. Topoisomerase inhibitors: Fluoroquinolone mechanisms of action and resistance. *Cold Spring Harb. Perspect. Med.* **2016**, *6*, a025320. <https://doi.org/10.1101/cshperspect.a025320>.
5. Aldred, K.J.; Kerns, R.J.; Osherooff, N. Mechanism of Quinolone Action and Resistance. *Biochemistry* **2014**, *53*, 1565–1574. <https://doi.org/10.1021/bi5000564>.
6. Coba-Males, M.A.; Lavecchia, M.J.; Alcívar-León, C.D.; Santamaría-Aguirre, J. Novel Fluoroquinolones with Possible Antibacterial Activity in Gram-Negative Resistant Pathogens: In Silico Drug Discovery. *Molecules* **2023**, *28*, 6929. <https://doi.org/10.3390/molecules28196929>.
7. Bush, N.G.; Diez-Santos, I.; Abbott, L.R.; Maxwell, A. Quinolones: Mechanism, lethality and their contributions to antibiotic resistance. *Molecules* **2020**, *25*, 5662. <https://doi.org/10.3390/molecules25235662>.
8. Agu, P.C.; Afiukwa, C.A.; Orji, O.U.; Ezech, E.M.; Ofoke, I.H.; Ogbu, C.O.; Ugwuja, E.I.; Aja, P.M. Molecular docking as a tool for the discovery of molecular targets of nutraceuticals in diseases management. *Sci. Rep.* **2023**, *13*, 13398. <https://doi.org/10.1038/s41598-023-40160-2>.
9. Berman, H.M.; Westbrook, J.; Feng, Z.; Gilliland, G.; Bhat, T.N.; Weissig, H.; Shindyalov, I.N.; Bourne, P.E. The Protein Data Bank. *Nucleic Acids Res.* **2000**, *28*, 235–242. <https://doi.org/10.1093/nar/28.1.235>.
10. Apweiler, R.; Bairoch, A.; Wu, C.H.; Barker, W.C.; Boeckmann, B.; Ferro, S.; Gasteiger, E.; Huang, H.; Lopez, R.; Magrane, M.; et al. UniProt: The Universal Protein knowledgebase. *Nucleic Acids Res.* **2003**, *32*, 115D–119. <https://doi.org/10.1093/nar/gkh131>.
11. Bilofsky, H.S.; Christian, B. The GenBank®genetic sequence data bank. *Nucleic Acids Res.* **1988**, *16*, 1861–1863. <https://doi.org/10.1093/nar/16.5.1861>.
12. Yang, J.; Zhang, Y. Protein structure and function prediction using I-TASSER. *Curr. Protoc. Bioinform.* **2015**, *52*, 5.8.1–5.8.15. <https://doi.org/10.1002/0471250953.bi0508s52>.
13. Waterhouse, A.; Bertoni, M.; Bienert, S.; Studer, G.; Tauriello, G.; Gumienny, R.; Heer, F.T.; De Beer, T.a.P.; Rempfer, C.; Bordoli, L.; et al. SWISS-MODEL: Homology modelling of protein structures and complexes. *Nucleic Acids Res.* **2018**, *46*, W296–W303. <https://doi.org/10.1093/nar/gky427>.
14. Kelley, L.A.; Mezulis, S.; Yates, C.M.; Wass, M.N.; Sternberg, M.J.E. The Phyre2 web portal for protein modeling, prediction and analysis. *Nat. Protoc.* **2015**, *10*, 845–858. <https://doi.org/10.1038/nprot.2015.053>.
15. Davis, I.W.; Leaver-Fay, A.; Chen, V.B.; Block, J.N.; Kapral, G.J.; Wang, X.; Murray, L.W.; Arendall, W.B.; Snoeyink, J.; Richardson, J.S.; et al. MolProbity: All-atom contacts and structure validation for proteins and nucleic acids. *Nucleic Acids Res.* **2007**, *35*, W375–W383. <https://doi.org/10.1093/nar/gkm216>.
16. Irwin, J.J.; Shoichet, B.K. ZINC—A free database of commercially available compounds for virtual screening. *J. Chem. Inf. Model.* **2005**, *45*, 177–182. <https://doi.org/10.1021/ci049714>.
17. Bell, E.W.; Zhang, Y. DockRMSD: An open-source tool for atom mapping and RMSD calculation of symmetric molecules through graph isomorphism. *J. Cheminform.* **2019**, *11*, 40. <https://doi.org/10.1186/s13321-019-0362-7>.
18. Pagadala, N.S.; Syed, K.; Tuszynski, J. Software for molecular docking: A review. *Biophys. Rev.* **2017**, *9*, 91–102. <https://doi.org/10.1007/s12551-016-0247-1>.
19. Trott, O.; Olson, A.J. AutoDock Vina: Improving the speed and accuracy of docking with a new scoring function, efficient optimization, and multithreading. *J. Comput. Chem.* **2009**, *31*, 455–461. <https://doi.org/10.1002/jcc.21334>.
20. Fàbrega, A.; Madurga, S.; Giralt, E.; Vila, J. Mechanism of action of and resistance to quinolones. *Microb. Biotechnol.* **2008**, *2*, 40–61. <https://doi.org/10.1111/j.1751-7915.2008.00063.x>.
21. El-Saghier, A.M.; Abosella, L.; Hassan, A.; Elakesh, E.O.; Bräse, S.; Abuo-Rahma, G.E.-D.A.; Aziz, H.A. Design, Synthesis, and In Silico Studies of New Norfloxacin Analogues with Broad Spectrum Antibacterial Activity via Topoisomerase II Inhibition. *Pharmaceuticals* **2025**, *18*, 545. <https://doi.org/10.3390/ph18040545>.
22. Rahimi, H.; Najafi, A.; Eslami, H.; Negahdari, B.; Moghaddam, M.M. Identification of Novel Bacterial DNA Gyrase Inhibitors: An In Silico Study. Available online: <https://pmc.ncbi.nlm.nih.gov/articles/PMC4962306/#sec1-3> (accessed on).

23. Hooper, D.C.; Jacoby, G.A. Topoisomerase inhibitors: Fluoroquinolone mechanisms of action and resistance. *Cold Spring Harb. Perspect. Med.* **2016**, *6*, a025320. <https://doi.org/10.1101/cshperspect.a025320>.
24. Emmerson, A.M. The quinolones: Decades of development and use. *J. Antimicrob. Chemother.* **2003**, *51*, 13–20. <https://doi.org/10.1093/jac/dkg208>.
25. Sharma, V.; Das, R.; Mehta, D.K.; Gupta, S.; Venugopala, K.N.; Mailavaram, R.; Nair, A.B.; Shakya, A.K.; Deb, P.K. Recent insight into the biological activities and SAR of quinolone derivatives as multifunctional scaffold. *Bioorg. Med. Chem.* **2022**, *59*, 116674. <https://doi.org/10.1016/j.bmc.2022.116674>.

**Disclaimer/Publisher's Note:** The statements, opinions and data contained in all publications are solely those of the individual author(s) and contributor(s) and not of MDPI and/or the editor(s). MDPI and/or the editor(s) disclaim responsibility for any injury to people or property resulting from any ideas, methods, instructions or products referred to in the content.